Int J Adv Manuf Technol (2015) 77:897–905
DOI 10.1007/s00170-014-6490-3

ORIGINAL ARTICLE

An analytical investigation of pad wear caused by the conditioner in fixed abrasive chemical–mechanical polishing

N. Y. Nguyen · Z. W. Zhong · Yebing Tian

Received: 5 June 2014 / Accepted: 9 October 2014 / Published online: 28 October 2014

Abstract Fixed abrasive chemical–mechanical polishing (CMP) is an efficient surface finishing method. The non-uniformity of substrates after polishing is one of the most interesting things in current trends in research. One of the reasons for the non-uniformity is pad wear. The pad in this polishing process has abrasive grains embedded on the surface. Researching on the pad wear will help improve the pad conditioning process to get a better pad surface. Some studies have used kinematic motion to show the correlation between the cutting path density and the pad wear. However, the effect of contact time between the conditioner's grains and the pad surface on the pad wear non-uniformity has not been integrated yet. In this research, an analytical model was established by combining of the kinematic motions and the contact time to investigate the pad wear non-uniformity. The results indicated that the cutting path density and the contact time near the pad center are more than that near the pad edge. They could be the main reasons of the non-uniformity of the pad wear. The model results showed a good agreement with experiments.

Keywords Fixed abrasive · Chemical–mechanical polishing · Kinematic motion · Cutting path density · Contact time

N. Y. Nguyen · Z. W. Zhong (✉)
School of Mechanical and Aerospace Engineering, Nanyang Technological University, 50 Nanyang Avenue, 639798 Singapore, Singapore
e-mail: MZWZHONG@ntu.edu.sg

N. Y. Nguyen
e-mail: nhuy001@e.ntu.edu.sg

Y. Tian (✉)
Singapore Institute of Manufacturing Technology, 71 Nanyang Drive, 638075 Singapore, Singapore
e-mail: ybtian@simtech.a-star.edu.sg

1 Introduction

Chemical–mechanical polishing is the only process that can provide both local and global planarization of a wafer [1]. However, environment problems when slurry is disposed and cost are reasons for using a fixed abrasive chemical–mechanical polishing (CMP) [2]. Fixed abrasive CMP has been used in manufacturing of optical components. It can produce surfaces with a high material removal rate with acceptable surface roughness [3]. Zhong et al. [4] indicate that it shortens the CMP time. Tian et al. [5] have shown better results of glass polishing by using the method instead of traditional surface finishing, which includes a loose abrasive lapping, a mechanical polishing, and the conventional chemical–mechanical polishing [5]. They also do research on various kinds of abrasive free slurry, with different operation parameters and in situ/ex situ conditioning and found out the optimum values for material removal rate and surface roughness [5–8].

In the CMP process, pad wear has an important effect on the uniformity of wafer substrates [9–11]. If the pad wear is not uniform, the cutting effect of the pad on the wafer surface is also not uniform [10, 12]. The better uniformity of the wafer surface could be also achieved by changing the thickness and stiffness of the subpad layers [3] combined with using a conditioner [13]. There are usually three main layers of the pad: the soft foam layer at the bottom for global planarization, the hard layer in the middle for pattern selectivity, and the abrasive layer on the top [3, 14]. The combination of thick sublayers of both the foam layer and the hard layer showed the best result in the uniformity of the wafer surface [3].

There are two main reasons that cause the pad wear: first, the contact behavior of the wafer and the pad, and second, the cutting grains of the conditioner. Some researchers have shown that the concavity of the polishing pad increased with conditioning time [15, 16]. Hooper et al. [17] have found out that the glazing is the highest at the center of the pad. Some other researchers have investigated the CMP process based on the kinematic of the cutting motion [10, 15, 18–26]. Lee et al. [10] studied a kinematical model of motions of the conditioner in the CMP process; however, the conditioner in their research is handled by a swing arm, not an oscillation motion in the radial direction. Chang et al. [15] also proposed a mathematical model based on a kinematic motion, but they assumed that "the oscillation velocity is neglected." Feng [19] established a model based on kinematical motion to research the pad wear caused by the conditioner in the CMP process with a soft pad. A function of conditioning density was developed based on trajectories generated by the conditioner's grains. However, the difference in speeds of the sweeping motion of the conditioner has not been investigated yet. Li et al. [20] developed a model for predicting the pad wear shape after conditioning. Their model was based on kinematic motion, but it used a surface element method to predict the pad shape. Yeh and Chen [21] also developed a model for predicting pad wear based on kinematic motion, but the conditioner in their model was a swing motion, not the oscillation motion. Baisie et al. [22] built up a model also based on kinematic motion of the conditioner to predict the pad wear, but the conditioner in the model did not oscillate. It moved from the pad center to the pad periphery. As it touched the pad periphery, it lifted up and moved back to its initial position to complete a whole cycle.

Researching the motion of the conditioner and the contact time between the grains and the pad surface plays an important role in predicting the pad wear [17, 16]. To our best knowledge, no study has yet reported the effects of combination of cutting path density and contact time between grains of the conditioner and the pad surface on the pad wear non-uniformity, especially in the fixed abrasive CMP process.

In this research, an analytical model for predicting the pad wear non-uniformity was developed. This model was based on a combination of kinematic motions of the conditioner's grains and the contact time between the grains and the pad surface. A program was written by using Fortran95 language. By using this program, the effects of both factors, the cutting path density and the contact time, on the pad wear non-uniformity can be investigated at the same time.

2 Motion of one abrasive grain of the conditioner

This study considered the motion of one grain of the conditioner on the pad surface. Figure 1 presents the schematic of motions of the pad and the conditioner in the CMP process.

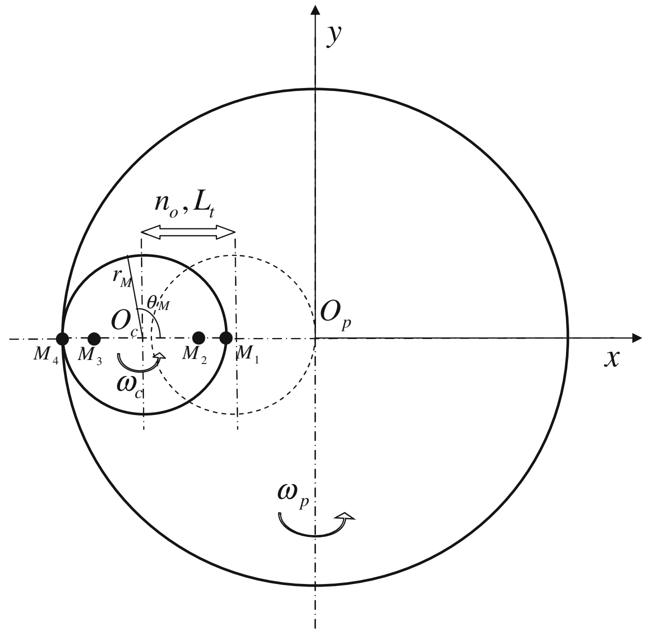

Fig. 1 Model of motions of the pad and the conditioner

The pad rotates with an angular velocity ω_p around the pad center O_p. The conditioner rotates with an angular velocity ω_c around the conditioner center O_c. The conditioner also oscillates in the X direction with a frequency n_o. The motion of one point M of the conditioner is investigated.

If the origin of the coordinate system is the conditioner center, the position of one grain is shown as:

$$\begin{cases} x^{'}(t) = r_M \cos(\omega_c t + \theta_M) \\ y^{'}(t) = r_M \sin(\omega_c t + \theta_M) \\ z^{'}(t) = ft \end{cases} \quad (1)$$

where $x'(t)$,$y'(t)$, and $z'(t)$ are the position of M in the coordinate system which has the origin at the conditioner center, r_M is the distance from M to the conditioner center, and θ_M is the initial location angle of M on the conditioner.

Actually, the origin is the pad center. Therefore, the position of M in the coordinate system is:

$$\begin{cases} x(t) = x^{'}(t) + L_t = r_M \cos(\omega_c t + \theta_M) + L_t \\ y(t) = y^{'}(t) = r_M \sin(\omega_c t + \theta_M) \\ z(t) = z^{'}(t) = ft \end{cases} \quad (2)$$

where $x(t)$, $y(t)$, and $z(t)$ are the position of point M with time t in the coordinate system which has the origin at the pad center, L_t is the distance between the conditioner center and the pad center, and f is the feed rate.

The equation of motion of point M can be described as [27]:

$$\begin{Bmatrix} x(t) \\ y(t) \\ z(t) \end{Bmatrix} = \mathrm{A}\cdot\mathrm{D}\cdot \begin{bmatrix} r_M \\ L_t \\ f \end{bmatrix} \quad (3)$$

A is the matrix expressing the rotation around the origin. D is the matrix expressing the rotation around the conditioner center and the translation from the conditioner center to the pad center.

$$\mathrm{A} = \begin{bmatrix} \cos(\omega_p t + \theta_p) & -\sin(\omega_p t + \theta_p) & 0 \\ \sin(\omega_p t + \theta_p) & \cos(\omega_p t + \theta_p) & 0 \\ 0 & 0 & 1 \end{bmatrix} \quad (4)$$

$$\mathrm{D} = \begin{bmatrix} \cos(\omega_c t + \theta_M) & 1 & 0 \\ \sin(\omega_c t + \theta_M) & 0 & 0 \\ 0 & 0 & t \end{bmatrix} \quad (5)$$

Table 1 Parameter list

R_p	Pad radius, 300 mm
R_c	Conditioner radius, 100 mm
(r_M,θ_M)	Grain initial location on the conditioner: $(0\leq\theta_M\leq2\pi)$, and $(70\leq r_M\leq100)$
θ_p	Angle of the first contact point on the pad
n_p	Pad rotation speed (+, CCW; −, CW) (rpm)
n_c	Conditioner rotation speed (+, CCW; −, CW) (rpm)
n_o	Conditioner oscillation frequency (stroke/min)
ω_p	Pad angular speed $(=2\pi\cdot n_p/60)$
ω_c	Wafer angular speed $(=2\pi\cdot n_c/60)$
ω_o	Conditioner oscillation speed $(=2\pi\cdot n_o/60)$
f	Feed rate

where ω_p,ω_c are the angle velocity of conditioner and pad, respectively, and θ_p is the angle of the first contact point on the pad. The parameters are summarized in Table 1.

The conditioner oscillates in the X direction. Assume L_t is a harmonic oscillation: $L_t=B\cos\omega_o t+C$, where ω_o is the oscillating velocity, and B and C are constants which are determined by the distance and the center position of the oscillation conditioner. If the center position is in the middle between the pad center and the pad edge, and the oscillation width is 70 mm, then $L_t=35\cos\omega_o t-150$.

Figure 2 presents the cutting path patterns which are created using different oscillation speeds: n_o. When the conditioner is stable, one grain of the conditioner only draws a simple trajectory path on the pad surface. The trajectory with the small value of the oscillation frequency (2 strokes/min) is smoother than that with a high frequency (15 strokes/min). It means that the pad surface may be conditioned better with a low oscillation frequency of the conditioner.

The trajectories of the grains also change when the pad and conditioner rotation speeds change, as shown in Fig. 3. The shape of the trajectory depends on the ratio of the speeds of the conditioner/pad, n_c/n_p. If the ratio n_c/n_p is the same, for example, 20/40 and 40/80, the shapes of trajectories are the same, but the consistence of those paths is different. Certainly, the consistence of the paths caused by the faster speeds (40/80) is more than that by the slower speeds.

3 Model development

To consider the effect of cutting path on the wearing rate of the pad, the pad surface is divided into small species (Fig. 4). The values of dx and dy were chosen based on the distance that the grain moved in one time step. For the time step of 0.001 s, the distance that the grain moved is plotted in Fig. 5. The frequency of the oscillation and the rotation speeds of the conditioner and the pad were $n_o=10$ strokes/min, $n_c=40$ rpm, and $n_p=40$ rpm, respectively. In each 0.001 s, the grain moved a small distance in both the X and Y directions. To consider the whole process, 12,000 steps of time were considered. As shown in Fig. 5, the distance that the grain moved in one time step is always smaller than 2 mm. Therefore, $dx=2$ mm and $dy=2$ mm were chosen. Also from Fig. 5, the cycle of the process with $n_o=10$ strokes/min, $n_c=40$ rpm, and $n_p=40$ rpm is 6 s.

There are many grains on the conditioner. Therefore, many cutting paths appear on the pad surface. Those grains used in calculating must represent the whole conditioner. The

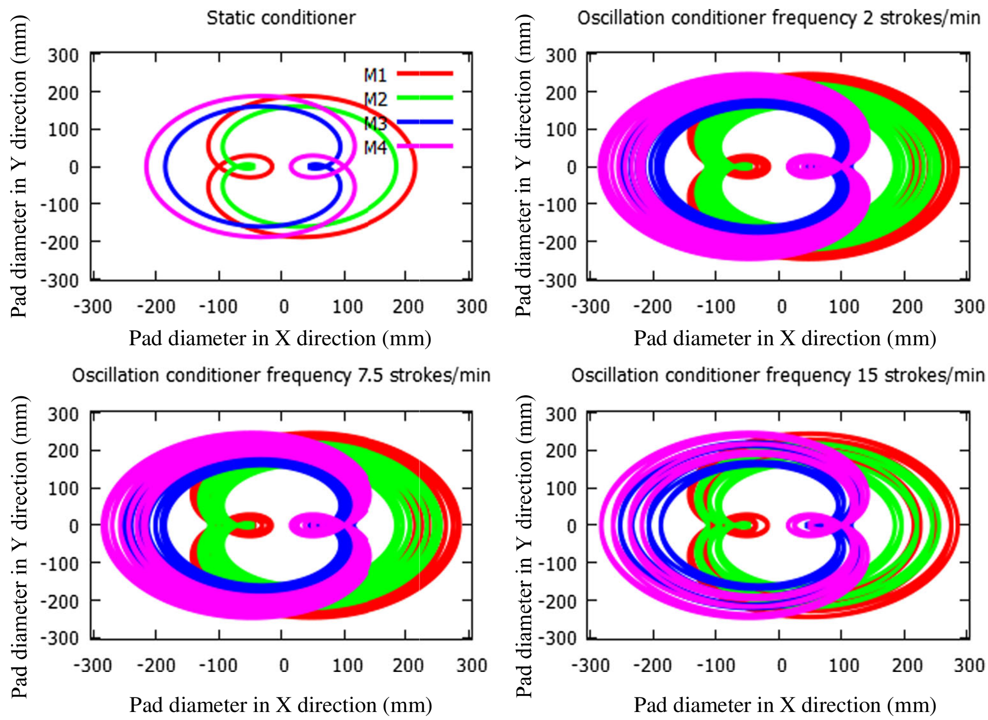

Fig. 2 Trajectories of four points of grains of the conditioner on the pad surface when the oscillation frequency changes

conditioner is divided into 180 parts (Fig. 4). The first and last grains on each part are chosen. The position of the first grain on each part is calculated based on the grain configuration of the conditioner. The distance between the first and last grains is about 10 mm. There are 21 grains on each part, used to draw their trajectories including the first grain, the last grain, and those grains between the first and last grains.

A program was written using Fortran95. The flowchart of the program is presented in Fig. 6. The position of one grain is calculated using Eq. 3. The Z coordinate of the pad surface is zero at the beginning. For each time the grain appears in one area, the Z coordinate of the area decreases by one unit. For example, at *n*th time step, if the position of the grain is at area A (i, j), the Z coordinate of area A (i, j) decreases by one unit. At (*n*+1)th time step, if the position of the grain is at area A (i +1, j), the Z coordinate of area A (i +1, j) decreases by one unit. However, if the position of the grain is still at area A (i, j) at (*n*+1)th time step, the Z coordinate of area A (i, j) decreases by one more unit. To ensure the symmetric of the pattern of the cutting paths of grains, at the beginning of each process, the pad and the conditioner contact at various positions. The program was run at 16 various positions. The program collected all the Z coordinates of all the areas of the pad surface after the process.

The Z coordinates of all the areas on the pad surface are actually the numbers of passes of the cutting paths of the conditioner grains. In this research, it can be called the Z coordinates of the pad surface. Consequently, the pad surface after the conditioning process can be estimated. However, they are not exactly the values of the pad surface after the conditioning process. Those values can be used to investigate the effects of the cutting path density and the contact time on pad wear at the same time.

4 Model verification and discussion

The pad wear was measured after polishing many times in experiments. The oscillation width and stroke were changed in each experiment. However, the final shape of the pad surface was always concave. The CMP machine used in this research was an Okamoto SPP-600S. The diameters of the pad and the conditioner are 600 and 200 mm, respectively. Figure 7 presents the positions for measuring the pad height. The pad was divided by six lines, and each line had 30 points. The pad height at each point was measured. The distribution of the values of the pad height at those points was standardized using Excel software.

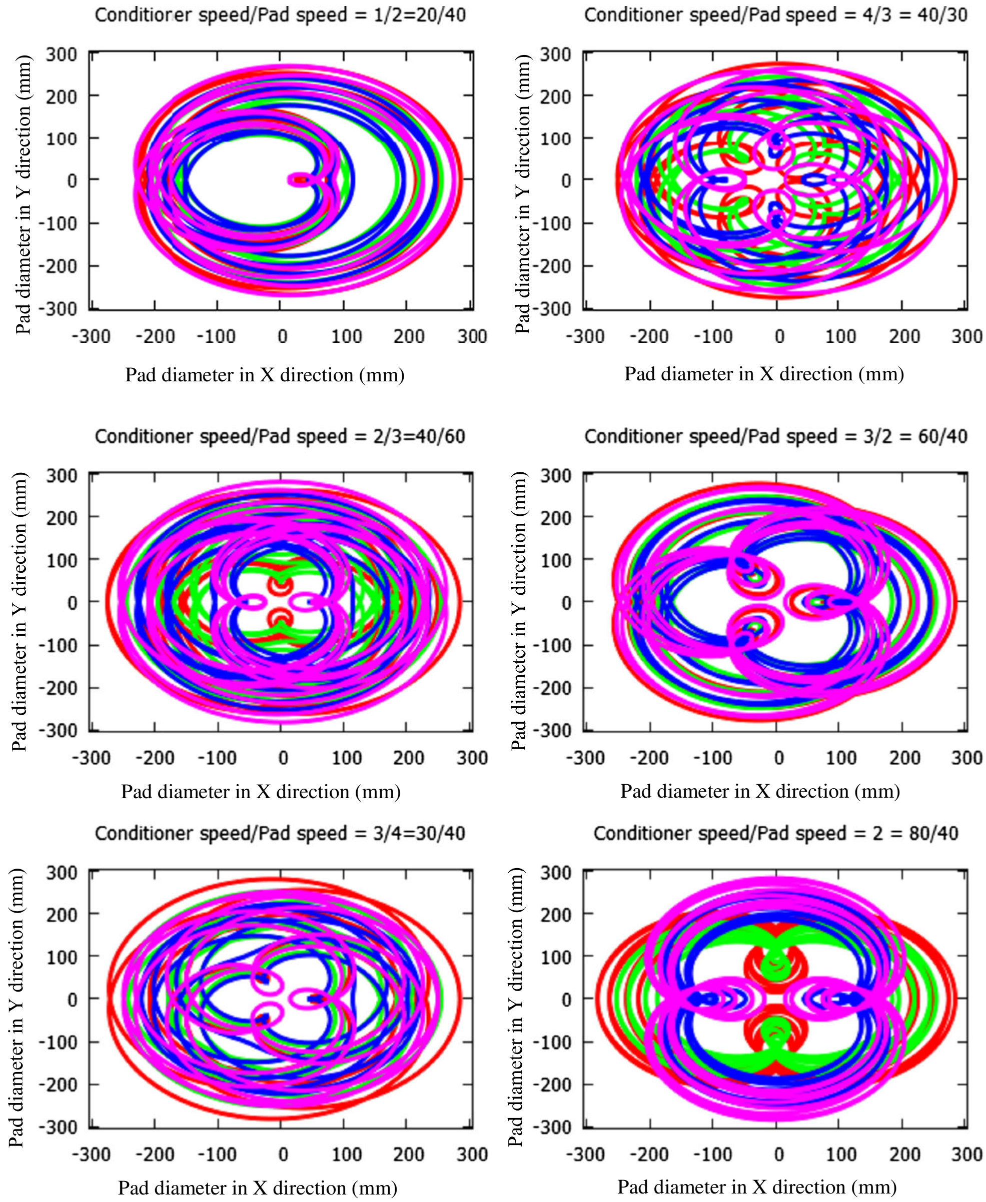

Fig. 3 Trajectories of four points of grains with different speeds of the conditioner and the pad

The equation for the standardized value is:

$$Z' = \frac{Z-\mu}{\sigma} \quad (6)$$

Where Z' is the standardized value, Z is the value that needs to be standardized, μ is the mean value of the distribution, and σ is the standard deviation of the distribution.

Similarly, the values of the Z coordinates of the pad surface from the model were also standardized. Both of standardizations were plotted as shown in Fig. 8a. There is a good agreement in the results from the model and the experiments (Fig. 8a). That means that the model is suitable for explaining the pad wear.

Moreover, the model investigated the effects of both the cutting path density and the contact time between the grains of the conditioner and the pad surface. The model in this study integrates the contact time, and it is called the contact time model. The model was compared with a non-contact time model. The non-contact time model was established when only the cutting path density was considered. For

Fig. 4 The conditioner geometry and the divided pad

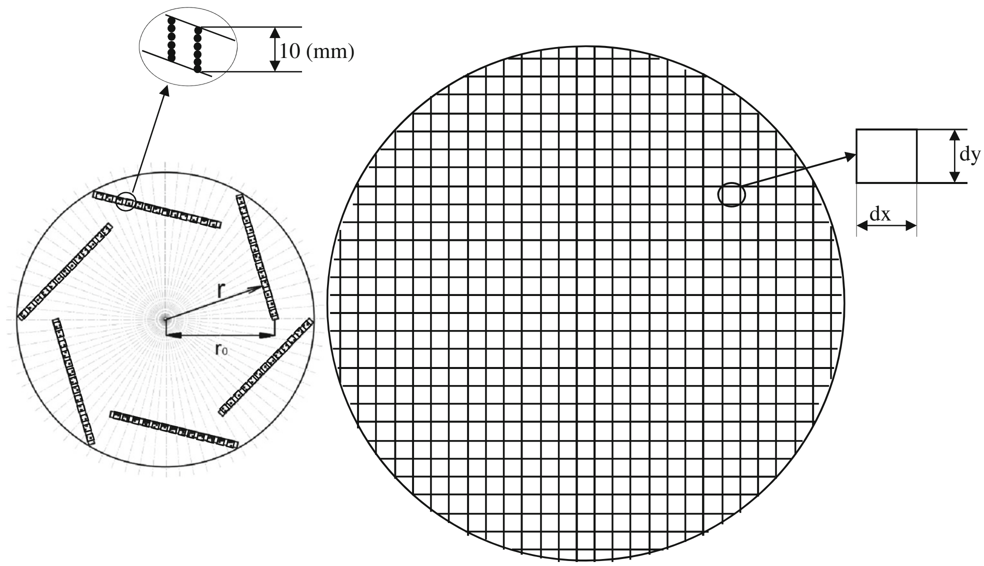

example, at nth time step, if the position of the grain is at area A (i, j), the Z coordinate of area A (i, j) decreases by one unit, and at $(n+1)$th time step, if the position of the grain is still at area A (i, j) the Z coordinate of area A (i, j) is unchanged. The difference of the standardization values of the Z coordinates of the pad surfaces between the two models is shown in Fig. 8b. The non-contact time model is symmetric, and the lowest value is in the middle between the pad center and the pad edge where the cutting path density is the largest. The pad wear that the non-contact time model predicted is different from the experiment results. Therefore, the contact time model is better than the non-contact time model in explaining the pad wear. From the contact time model, one conclusion can be suggested that the pad wear is the results of both the cutting path density and the contact time between the grains of the conditioner and the pad surface.

5 Conclusion

The research showed the two main reasons that caused the non-uniformity pad wear in the CMP process. They are the distribution of cutting path density and the

Fig. 5 Distances that the grain moves in one time step in the X and Y directions

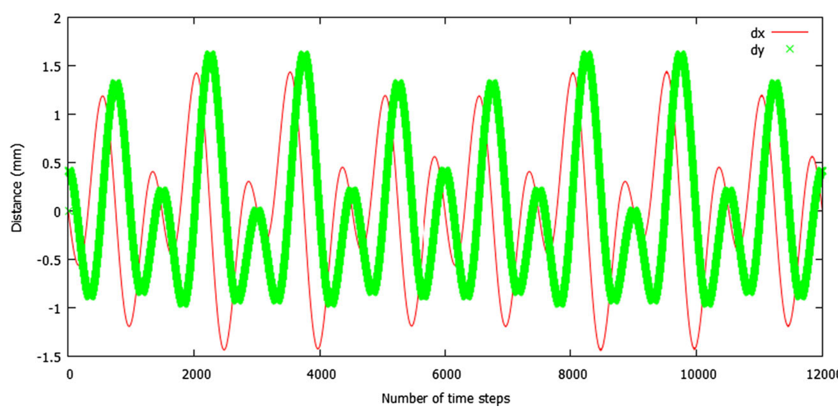

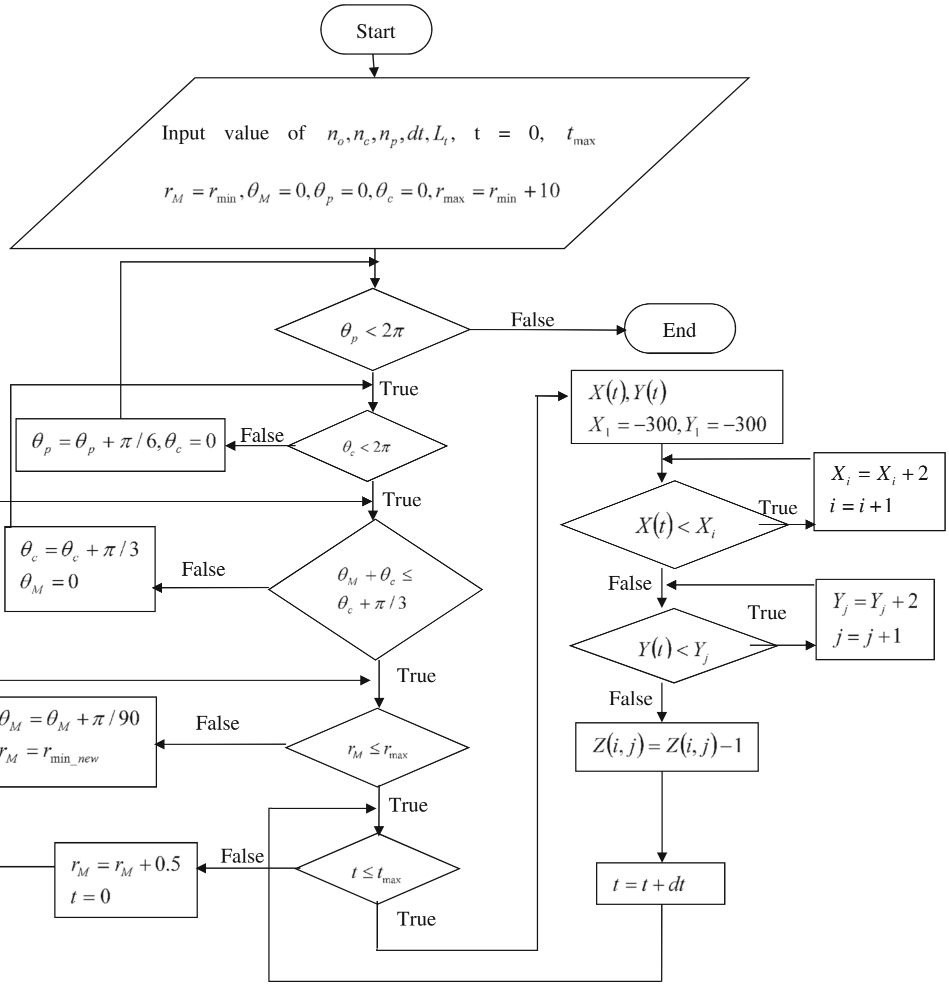

Fig. 6 Flowchart of the program for calculating the Z coordinate of the pad surface

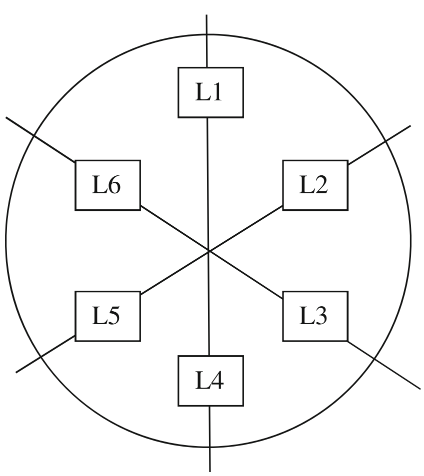

Fig. 7 Measured positions for the pad height on the pad in experiments

contact time between the conditioner and the pad surface. The motion of the conditioner in this research was a combination of two motions: rotation and oscillation. When the cutting path density and the contact time increase, the pad wear rate increases. The cutting path density and the contact time near the pad center are more than that near the pad edge. An analytical model based on the two factors was proposed for the fixed abrasive pad. The results from the analytical model showed a good agreement with the experiment results. From the effects of the cutting path density and the contact time on the pad wear, a mathematical model could be developed to calculate and improve the uniformity of the pad wear.

Fig. 8 Standardization values of the *Z* coordinates of the pad surface of the model; **a** comparing to the experiment data and **b** comparing to the non-contact time model

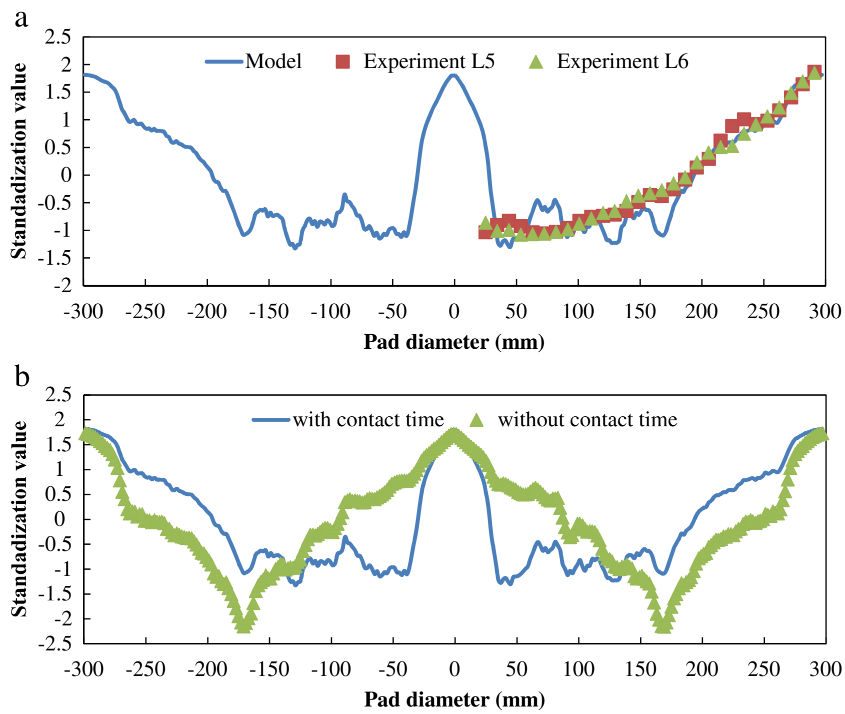

Acknowledgments This research was financially sponsored by the Agency for Science, Technology and Research of Singapore via Singapore Institute of Manufacturing Technology (SIMTech) Project Grants C10-M-035 and P11-M-058U. The authors would like to thank the Centre for Optical and Laser Engineering, the School of Mechanical and Aerospace Engineering, Nanyang Technological University, for providing a PhD scholarship.

References

1. Kim HJ (2013) Tribological approaches to material removal rate during chemical mechanical polishing. Met Mater Int 19(2):335
2. Enomoto T, Satake U, Fujita T, Sugihara T (2013) Spiral-structured fixed-abrasive pads for glass finishing. CIRP Ann Manuf Technol 62(1):311–314. doi:10.1016/j.cirp.2013.03.011
3. van der Velden P (2000) Chemical mechanical polishing with fixed abrasives using different subpads to optimize wafer uniformity. Microelectron Eng 50(1–4):41–46
4. Zhong ZW, Tian YB, Ng JH, Ang YJ (2013) Chemical mechanical polishing (CMP) processes for manufacturing optical silicon substrates with shortened polishing time. Mater Manuf Process 29(1): 15–19
5. Tian YB, Zhong ZW, Lai S, Ang Y (2013) Development of fixed abrasive chemical mechanical polishing process for glass disk substrates. Int J Adv Manuf Technol 68(5–8):993–1000
6. Tian YB, Zhong ZW, Ng JH (2013) Effects of chemical slurries on fixed abrasive chemical–mechanical polishing of optical silicon substrates. Int J Precis Eng Manuf 14(8):1447–1454
7. Tian YB, Ang YJ, Zhong ZW, Xu H, Tan R (2013) Chemical mechanical polishing of glass disk substrates: preliminary experimental investigation. Mater Manuf Process 28(4):488–494
8. Zhong ZW, Tian YB, Ang Y, Wu H (2012) Optimization of the chemical mechanical polishing process for optical silicon substrates. Int J Adv Manuf Technol 60(9–12):1197–1206
9. Liao XY, Zhuang Y, Borucki LJ, Cheng J, Theng S, Ashizawa T, Philipossian A (2013) Effect of pad surface micro-texture on removal rate during interlayer dielectric chemical mechanical planarization process. Japanese Journal of Applied Physics 52 (1). doi:10.7567/jjap.52.018001
10. Lee S, Jeong S, Park K, Kim H, Jeong H (2009) Kinematical modeling of pad profile variation during conditioning in chemical mechanical polishing. Jpn J Appl Phys 48(12):126502–126505
11. Baisie E, Li ZC, Zhang XH (2013) Design optimization of diamond disk pad conditioners. Int J Adv Manuf Technol 66(9–12):2041–2052
12. Tso P-L, Ho S-Y (2007) Factors influencing the dressing rate of chemical mechanical polishing pad conditioning. Int J Adv Manuf Technol 33(7–8):720–724
13. Achuthan K, Curry J, Lacy M, Campbell D, Babu S (1996) Investigation of pad deformation and conditioning during the CMP of silicon dioxide films. J Electron Mater 25(10):1628–1632
14. Kim H, Kim H, Jeong H, Seo H, Lee S (2003) Self-conditioning of encapsulated abrasive pad in chemical mechanical polishing. J Mater Process Technol 142(3):614–618. doi:10.1016/S0924-0136(03)00641-1
15. Chang O, Kim H, Park K, Park B, Seo H, Jeong H (2007) Mathematical modeling of CMP conditioning process. Microelectron Eng 84(4):577–583
16. Y-y Z, Davis EC (1999) Variation of polish pad shape during pad dressing. Mater Sci Eng B 68(2):91–98. doi:10.1016/S0921-5107(99)00423-7
17. Hooper B, Byrne G, Galligan S (2002) Pad conditioning in chemical mechanical polishing. J Mater Process Technol 123(1):107–113
18. Zhao D, Wang T, He Y, Lu X (2013) Kinematic optimization for chemical mechanical polishing based on statistical analysis of particle trajectories. IEEE Trans Semicond Manuf 26(4):556–563

19. Feng T (2007) Pad conditioning density distribution in CMP process with diamond dresser. IEEE Trans Semicond Manuf 20(4):464–475
20. Li Z, Baisie EA, Zhang X (2012) Diamond disc pad conditioning in chemical mechanical planarization (CMP): a surface element method to predict pad surface shape. Precis Eng 36(2):356–363
21. Yeh H-M, Chen K-S (2010) Development of a pad conditioning simulation module with a diamond dresser for CMP applications. Int J Adv Manuf Technol 50(1–4):1–12
22. Baisie EA, Li Z, Zhang X (2013) Pad conditioning in chemical mechanical polishing: a conditioning density distribution model to predict pad surface shape. Int J Manuf Res 8(1):103–119
23. Zhao D, He Y, Wang T, Lu X (2012) Effect of kinematic parameters and their coupling relationships on global uniformity of chemical–mechanical polishing. IEEE Trans Semicond Manuf 25(3):502–510
24. Feng T (2007) Nonuniformity of wafer and pad in CMP: kinematic aspects of view. IEEE Trans Semicond Manuf 20(4):451–463
25. Kim H, Jeong H (2004) Effect of process conditions on uniformity of velocity and wear distance of pad and wafer during chemical mechanical planarization. J Electron Mater 33(1):53–60. doi:10.1007/s11664-004-0294-4
26. Hocheng H, Tsai H, Tsai M (2000) Effects of kinematic variables on nonuniformity in chemical mechanical planarization. Int J Mach Tools Manuf 40(11):1651–1669
27. Zhou LB, Shimizu J, Shinohara K, Eda H (2003) Three-dimensional kinematical analyses for surface grinding of large scale substrate. Precis Eng J Int Soc Precis Eng Nanotechnol 27(2):175–184. doi:10.1016/s0141-6359(02)00225-8